J Biol Phys (2007) 33:485–498
DOI 10.1007/s10867-008-9104-1

ORIGINAL PAPER

In Silico Kinetic Study of the Glucose Transporter

G. L. Alonso · D. A. González

Received: 29 October 2007 / Accepted: 4 July 2008 /
Published online: 15 August 2008
© Springer Science + Business Media B.V. 2008

Abstract Glucose transport in plasma membranes is the prototypic example of facilitated diffusion through biological membranes, and transport in erythrocytes is the most widely studied. One of the oldest and simplest models describing the kinetics of the transport reaction is that of alternating conformers, schematized in a cycle of four partial reactions where glucose binds and dissociates at two opposite steps, and the transporter undergoes transconformations at the other two opposite steps. The transport kinetics is entirely defined by the forward and backward rate constants of the partial reactions and the glucose and transporter concentrations at each side of the membrane, related by the law of mass action. We studied, *in silico*, the effect of modifications of the variables on the transient kinetics of the transport reaction. The simulations took into account thermodynamic constraints and provided results regarding initial velocities of transport, maximal velocities in different conditions, apparent influx and efflux affinities, and the turnover number of the transporter. The results are in the range of those experimentally reported. Maximal initial velocities are obtained when the affinities of the ligand for the transporter are the same at the extra- and intracellular binding sites and when the equilibrium constants of the transconformation steps are equal among them and equal to 1, independently of the obvious effect of the increase of the rate constant values. The results are well adjusted to Michaelis–Menten kinetics. A larger initial velocity for efflux than for uptake described in human erythrocytes is demonstrated in a model with the same dissociation constants at the outer and inner sites of the membrane. The larger velocities observed for uptake and efflux when transport occurs towards a glucose-containing *trans* side can also be reproduced with the alternating conformer model, depending on how transport velocities are measured.

Keywords Facilitated diffusion · Glucose transport · Kinetics

G. L. Alonso (✉) · D. A. González
Department of Biophysics, School of Dentistry, University of Buenos Aires,
M. T. de Alvear 2142, 1122 Buenos Aires, Argentina
e-mail: alonso@biofis.odon.uba.ar

1 Introduction

Glucose transport in plasma membranes is the prototypic example of facilitated diffusion through biological membranes. The transport is mediated by a family of membrane proteins (GLUTs). In turn, glucose transport through the erythrocyte plasma membrane is the most widely studied model of glucose transport. It has particular characteristics, such as those described as asymmetry and a *trans* effect [1–3]. One of the oldest and simplest models describing facilitated diffusion [4] is a four-step cycle of alternating conformers between the extracellular (e) and intracellular (i) compartments (Fig. 1): (1) The ligand (L) binds to the transporter (T) at one side of the membrane. (2) The T–L complex transconforms so that L now faces the opposite side. (3) L dissociates from T–L. (4) Free T undergoes another transconformation to reorient its L binding site and reinitiate the cycle. Results from experimental studies are usually adjusted by Michaelis–Menten kinetics, which allows calculations of the maximal transport velocity (V_m) and the apparent affinity (K_{mapp}) of the ligand for the transporter at each side of the membrane.

The development of the ^{18}F-fluorodeoxyglucose–positron emission tomography method for diagnosis of tumor metastasis added interest to the study of the kinetics of glucose transport in plasma cell membranes [5].

As far as we know, a detailed study of the effect of the relationships between the rate constants of the partial steps of the model on the overall kinetics of the cycle has not been reported. These considerations motivated the present study.

2 Methods

A scheme simulating the exchange of a solute between extracellular (e) and intracellular (i) compartments is shown in Fig. 2. At the limiting membrane, exchange proceeds through the partial steps of the reaction cycle shown in Fig. 1. Both compartments have the same volume. The system simulates a 50% (v/v) erythrocyte suspension. "Te" species belong to the "e" compartment, while "Ti" species belong to the "i" compartment.

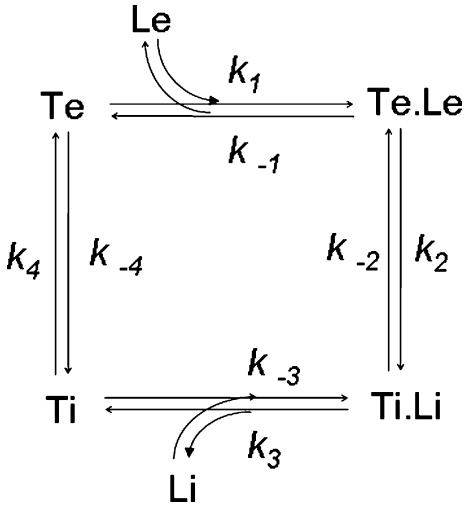

Fig. 1 Model of alternating conformers for facilitated diffusion. The transporter (*T*) alternates between two conformational states, Te and Ti, whose binding sites for the ligand (*L*) face the extracellular (e) and intracellular (i) medium, respectively. The equilibrium constants of the four partial reactions are defined by (1)

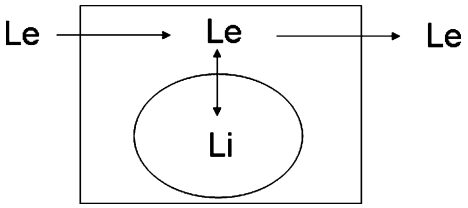

Fig. 2 Ligand distribution between extra- and intracellular compartments. Simulations assume a constant external ligand concentration ([Le]) buffered by instantaneous exchange with a large environment. Both compartments are separated by a membrane where the transport of the ligand occurs through the reactions schematized in Fig. 1. Unless otherwise indicated, for uptake reactions, the initial [Li] value equals zero and increases with time, and for efflux reactions, [Le] equals 0 and the initial [Li] value decreases with time

The model describes an open system where an extracellular ligand (Le) is maintained at constant concentration in instantaneous equilibrium with the environment. The concentration of the species is expressed in molar units (M, mM, or μM) and the transport velocities in millimolar per second. Both uptake and efflux of the ligand into and out of the intracellular compartment were analyzed. For uptake reactions, [Le] is maintained constant at different values in the low millimolar range and [Li] increases. For efflux analyses, [Le] is held at a constant value of zero; efflux starts from a given [Li] value which decreases during transport.

The cycle is reversible and fully described by the set of rate constants (k) defining the equilibrium constants (K) of each partial step (Fig. 1):

$$K_i = k_i / k_{-i}. \tag{1}$$

Since in equilibrium [Le] = [Li], the following thermodynamic constraint applies:

$$K = K_1 \times K_2 \times K_3 \times K_4 = 1. \tag{2}$$

The transient evolution of all the species of the model (Fig. 1) was followed, applying the set of differential equations given in Appendix 1. The concentration values of the species were calculated for different cumulative reaction times with a computer program [6] adapted to Borland–Delphi software.

Uptake and efflux analyses were made under several conditions where the dissociation constants in partial reactions 1 and 3 (Fig. 1) were either equal or different. The initial values of the species and the particular rate constant values are given under Section 3 for the different analyses.

Graphs were plotted with a Sigma-Plot 10.0 software. Linear and nonlinear regressions are calculated with fitting programs included in the software.

3 Results and Discussion

Our first purpose was to choose a set of rate constants and equilibrium constants to adequately reproduce results within the range of those experimentally obtained by several authors [1, 2, 7, 8].

3.1 Analyses with Equal Dissociation Constants of the Te–Le and Ti–Li Complexes

The dissociation constants of the ligand from the external (K_{De}) and internal (K_{Di}) sides of the membrane were first chosen:

$$K_{De}=K_{Di} = 1 \text{ mM}.$$

From (1):

$$K_1=1/K_{De} \text{ and } K_3=K_{Di}. \tag{3}$$

The numerical value was chosen taking into account the general agreement in the literature that the apparent affinity of glucose for the transporter lies in the low millimolar range near the glucose concentrations of mammalian extracellular fluids [1].

3.1.1 Equal Kinetic Constants for both Transconformation Steps: An Uptake Analysis and Definition of Initial Velocities (V_0)

For the sake of simplicity, we first choose:

$$k_2=k_{-2}=k_4=k_4, \text{ therefore } K_2=K_4.$$

Figure 3 shows the results of the transient evolution of species Li (Fig. 3a) and T (Fig. 3b) towards equilibrium. The rate constant values used are given in the legend. They adjust (1) and (2). Figure 3c shows the increase in [Li] during the first milliseconds; after a short lag, the transport reaction approaches linearity. The slope is the initial uptake velocity, which is calculated as:

$$V_0=[\text{Li}]_{5\text{ ms}} - [\text{Li}]_{4\text{ ms}}. \tag{4}$$

Similarly, the decrease of [Li] in efflux reactions was measured during the first milliseconds, after a short lag, when the transport reaction approached decreasing linearity (results not shown). The initial efflux velocities will be calculated with:

$$V_0=[\text{Li}]_{4\text{ ms}} - [\text{Li}]_{5\text{ ms}}. \tag{5}$$

In Fig. 3, the initial uptake velocity was $V_0 = 0.199$ mM/s.

3.1.2 Effect of the Transconformation Rate Constants k_2, k_{-2}, k_4, and k_{-4} on the Overall Transport

Keeping $K_{De}=K_{Di}=1$ mM, $K_1=1/K_3$, and according to (2) we should either have $K_2 = K_4 = 1$ (Section 3.1.2.1) or $K_2 \neq K_4$ related by $K_2 = 1/K_4$ (Section 3.1.2.2).

3.1.2.1 Uptake with Various Equal Transconformation Rate Constants: $k_2 = k_{-2} = k_4 = k_{-4} = k_i$

Figure 4 shows the transient evolution of "L" accumulation in the "i" compartment as a function of time (a) and the initial velocities of transport (b) for various k_i values.

The initial transport velocity increases up to a maximum limited by the rate constants k_1 and k_3 (Fig. 4b).

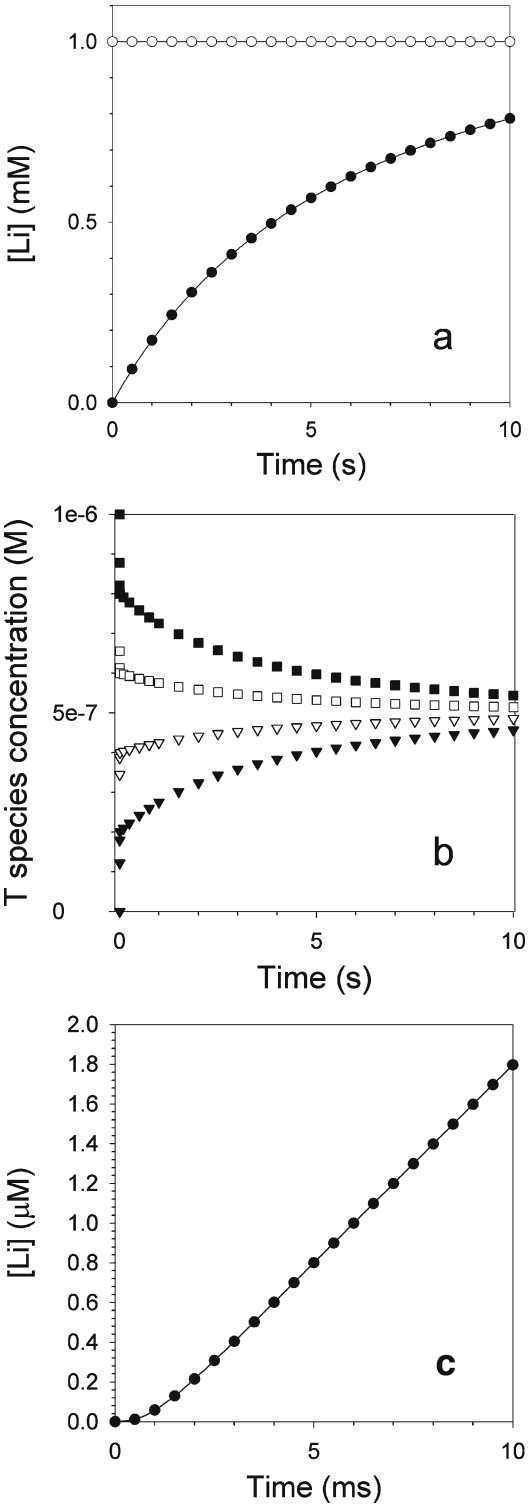

Fig. 3 Ligand uptake under the following simulation conditions. Initial conditions: (*open circles*) [Le] = 1 mM; (*open squares*) [Te] = (*filled squares*) [Ti] = 1 μM; (*open inverted triangles*) [Te–Le] = (*filled inverted triangles*) [Ti–Li] = (*filled circles*) [Li] = 0. Rate constants: $k_1 = k_{-3} = 1e6\ M^{-1}\ s^{-1}$; $k_{-1} = k_2 = k_{-2} = k_3 = k_4 = k_{-4} = 1e3\ s^{-1}$. **a** Time course of uptake up to 10 s. **b** Transient evolution of the T species along 10 s. **c** Initial transport velocity

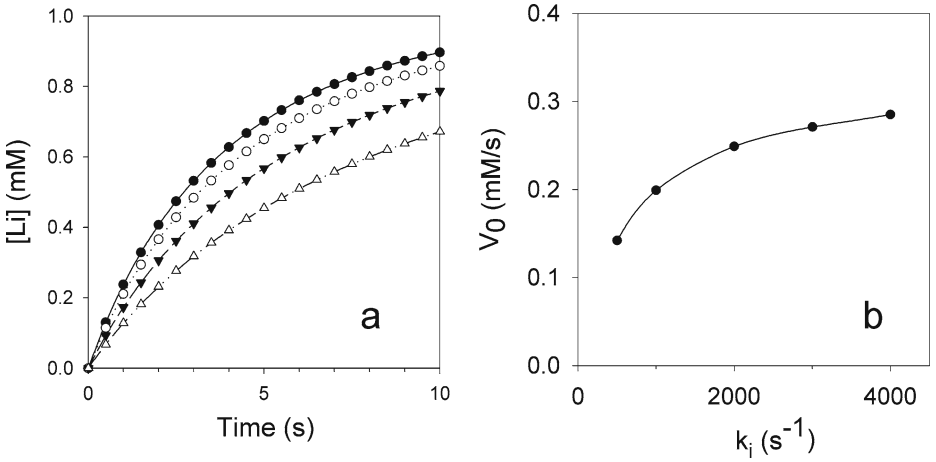

Fig. 4 Effect of the rate constant values of the transconformation steps on the uptake transport reaction. **a** Time course of L uptake up to 10 s for several values of the rate constants of the transconformation steps. Initial conditions and rate constants were as in Fig. 3 except k_i (s^{-1}) = $k_2 = k_{-2} = k_4 = k_{-4}$ = 500 (*open inverted triangles*), 1,000 (*filled inverted triangles*), 2,000 (*open circles*), or 4,000 (*filled circles*). **b** Initial velocities of the uptake reactions as a function of k_i values

3.1.2.2 Uptake and Efflux with Different Transconformation Equilibrium Constants

$K_2 = 1/K_4$; therefore, $k_2/k_{-2} = k_{-4}/k_4$, meaning that either both transconformations favor "e→i" reactions with similar driving forces or both favor the opposite reactions "i→e", also with similar driving forces. This implies that asymmetries between influx and efflux are expected to appear.

In Fig. 5a, k_{-2} and k_4 were maintained equal and constant, and uptake and efflux initial velocities were measured as a function of k_2 and k_{-4}, which were increased in parallel. The figure shows the effect of the increase of the driving forces of the reactions towards the "i" species.

In Fig. 5b, the opposite conditions are used. k_2 and k_{-4} are maintained constant, and uptake and efflux initial velocities are measured as a function of the parallel increase of k_{-2} and k_4 The figure shows the effect of the increase of the driving forces of the reactions towards the "e" species.

In Fig. 5c, the initial uptake and efflux velocities are expressed as functions of the fractions of each "i→e" rate constant relative to an invariant sum of the forward and backward rate constants of the same reaction ($V_0 = f(k_{-2}/(k_2 + k_{-2}) = k_4/(k_4 + k_{-4})$), where $k_2 + k_{-2} = k_4 + k_{-4} = 2{,}000\ s^{-1}$. Similar analyses using the "e→i" rate constants as independent variables yielded the mirror image of the figure (not shown).

Taking together Figs. 4 and 5, where similar affinities of the ligand for the transporter on both sides of the membrane are assumed, we conclude that the increase of the initial velocities is obtained by an appropriate combination of two factors. (1) the absolute rate constant values of the transconformation reactions (Fig. 4) and (2) the approach of the equilibrium constants of these partial steps to their equality and to 1 (Fig. 5). Calling *cis* transport that flowing in favor of the increase of the independent variable and *trans* transport that flowing in the opposite direction, Fig. 5a, b shows that *trans* transport always occurs at maximal velocity when $K_2 = K_4 = 1$. In contrast, *cis* transports increase upon the increase

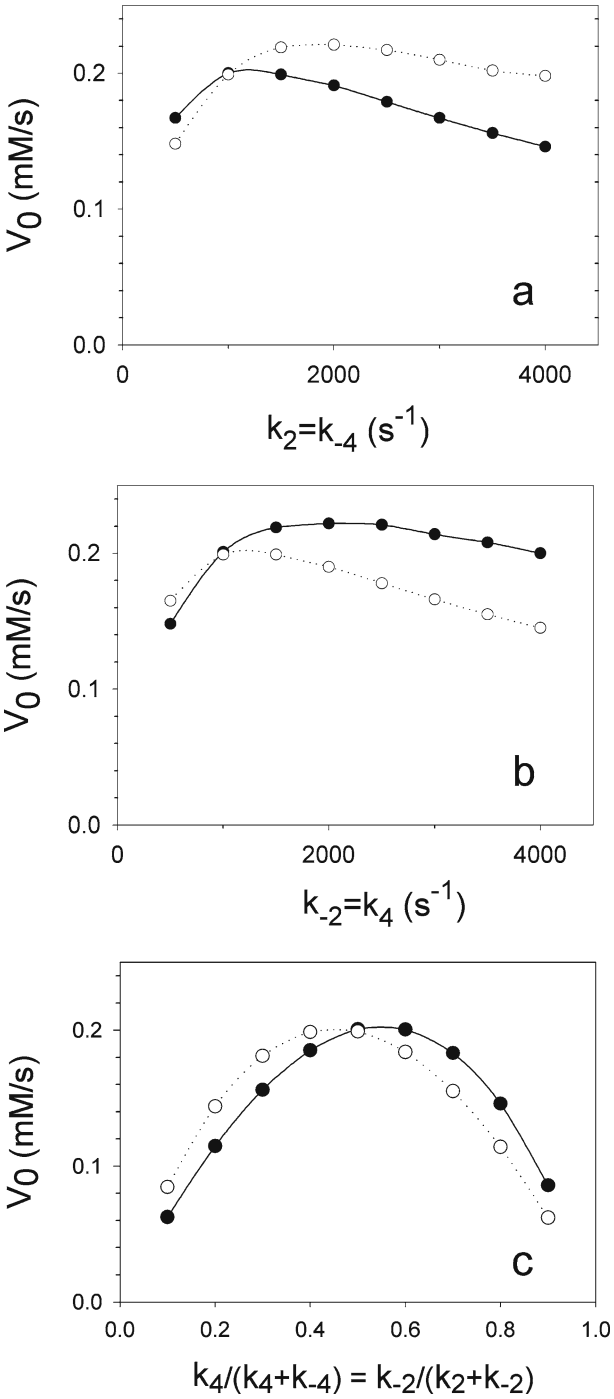

Fig. 5 Uptake (*open circles*) and efflux (*filled circles*) with transconformation equilibrium constants different from 1. For uptake reactions, [Le] is held constant at 1 mM, while [Li] increases with time. For efflux reactions, [Le] is held constant at 0 and $[Li]_0$ is initially set at 1 mM, and subsequently decreases with time. Since $K_{De} = K_{Di} =$ 1 mM was used, it should be $K_2 = 1/K_4$, meaning that $k_2/k_{-2} = k_{-4}/k_4$. **a** V_0 for uptake and efflux as a function of $k_2 = k_{-4}$, with $k_{-2} = k_4 = 1{,}000\ s^{-1}$. **b** V_0 for uptake and efflux as a function of $k_{-2} = k_4$, with $k_2 = k_{-4} = 1{,}000\ s^{-1}$. **c** V_0 for uptake and efflux as a function of $k_{-2}/(k_2 + k_{-2}) = k_4/(k_4 + k_{-4})$

of the independent rate constants, which give rise to the appearance of asymmetries between the initial velocities of influx and efflux.

3.1.3 Dependence of the Initial Velocities on the Transported Solute Concentration

Michaelis–Menten (M–M) kinetics for enzyme reactions [9] has been usually applied to transport reactions [1, 10]. To compare the present results with those from experiments analyzed with M–M kinetics, the initial transport velocities were calculated for various initial ligand concentrations, and M–M kinetics was applied to the results. Differences between the true affinities of the ligand for the transporter sites and the obtained K_m values are expected. The true affinity of the ligand for the outer transport site (reaction no. 1, Fig. 1) is the ligand concentration saturating one half of the sites, in equilibrium, defined by the law of mass action as the dissociation constant of the Te.Le complex. In contrast, the K_m value of the transport reaction is the ligand concentration yielding one half of the maximal initial transport velocity, which can be affected by other several factors, namely, the relative values of the forward rate constants k_1, k_2, and k_3, and the lack of an instantaneous equilibrium between the transporter and the ligand through reactions no. 1 and no. 2 to give the productive complex (Ti.Li) of the Li species.

3.1.3.1 The Behavior of the Model Adjusts to Michaelis–Menten Kinetics

The initial velocity of the uptake transport reaction was simulated for various [Le]. All other conditions were as in Fig. 3. The results are shown in Fig. 6. The data in Fig. 6a are adjusted with the M–M equation ($V_0 = V_m \times [L]/(K_m + [L])$). The double reciprocal plot of the data lies on a straight line (Fig. 6b). The figures show that the M–M analysis for enzyme kinetics applies to the alternating conformer model of facilitated diffusion. The maximal initial velocity (V_m) and the apparent Michaelis constant (K_{mapp}) are calculated from the figures either by non-

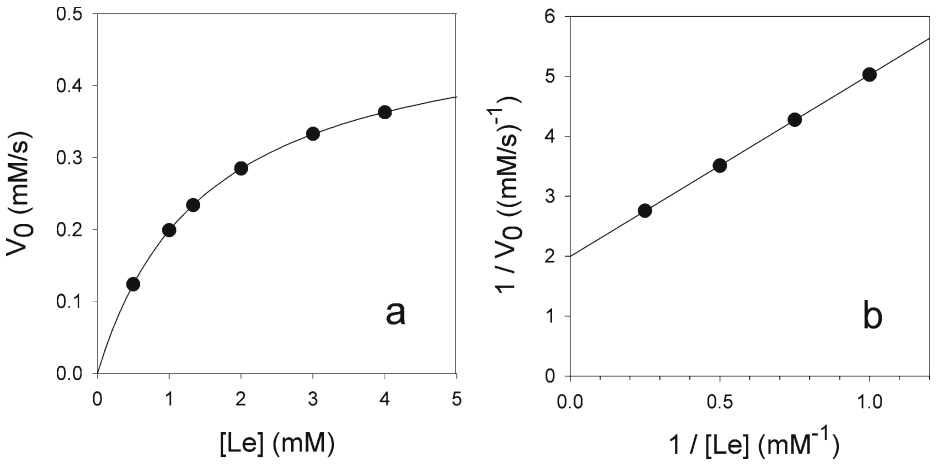

Fig. 6 Initial uptake velocity as a function of the concentration of the transported solute. **a** $V_0 = f([Le])$ The rate constant values and the initial conditions for the analyses were as in Fig. 3, except for the use of different $[Le]_0$, given in the abscissa. **b** Double reciprocal plot of the data

linear regression from Fig. 6a or by linear regression from Fig. 6b, with similar results:

$$V_m = 0.50 \text{ mM/s},$$

$$K_{mapp} = 1.51 \text{ mM}.$$

The values are within the range of experimental data obtained for glucose uptake in glucose-depleted human erythrocytes [2, 8]. The apparent K_m value is generally taken as an index of the affinity of the outer binding site for the ligand. Note the difference between the apparent K_m value obtained with the Michaelian analysis and the data used in the simulations for the affinity of the ligand to the external site (K_{De} = 1 mM).

The turnover rate of the transporter can also be calculated from data shown in Fig. 6:

$$\tau^{-1} = V_m/[T]_{total} = (0.5 \text{ mM/s})/2 \text{ μM} = 250 \text{ s}^{-1}.$$

The value is also within the range of experimental results [11].

3.1.3.2 Transport Asymmetry

It has been reported that maximal initial velocities (V_m) of glucose transport in human erythrocytes is five to 10 times larger for efflux than for influx [1, 12]. A larger, but less than two times, efflux than influx transport velocity is shown in Fig. 5b. To further enhance this effect, the driving forces of the "e→i" transconformations were increased, making $k_{-2}/k_2 = k_4/k_{-4} = 10$. The results are analyzed with M–M kinetics to compare with other analyses from experimental data [1, 12]. Figure 7a shows the influx and efflux

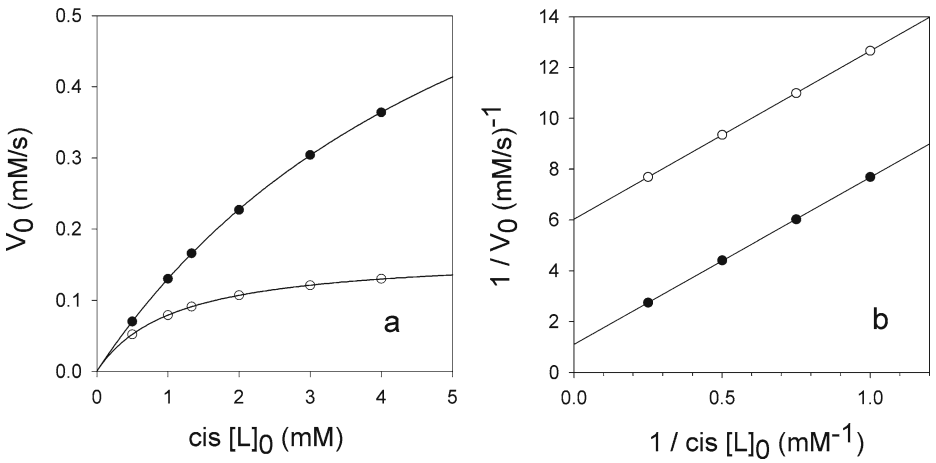

Fig. 7 Transport asymmetry. **a** The initial velocities of uptake and efflux transport reactions are shown as functions of the concentrations of the transported solute. Rate constant values are as in Fig. 3, except $k_{-2} = k_4$ = 1e4. Initial concentrations were: $[Te–Le]_0$ = $[Ti–Li]_0$ = 0, $[Te]_0$ = 1.818 μM, $[Ti]_0$ = 0.182 μM, and the inner and outer $[L]_0$ values as follows: For uptake (*open circles*), $[Le]_0$ is given in the abscissa, $[Li]_0$ = 0 and progressively increases, and initial velocities were calculated with (4). For efflux (*filled circles*), $[Li]_0$ is given in the abscissa and progressively decreases, $[Le]_0$ = 0 and remains constant along the reaction, and initial velocities were calculated with (5). **b** Double reciprocal plot of the data

Table 1 Asymmetry between uptake and efflux

	V_m(mM/s)	K_{mapp}(mM)
Efflux	0.90	5.91
Influx	0.17	1.13

V_m and K_m values were calculated from data shown in Fig. 7.

initial velocities of transport as a function of the *cis* initial [L]. Figure 7b shows the double reciprocal plot of the data.

Table 1 shows the calculated V_m and K_{mapp} values for efflux and influx. The results reproduce the asymmetry experimentally observed in human erythrocyte membranes [1, 12]. The ratio between the maximal initial velocities of efflux and influx is 5.3. The table also shows the large difference between K_{mapp} (efflux) calculated with M–M kinetics (5.9 mM) and the true affinity of the ligand for the inner site (1 mM). K_{mapp} derived from our results shown in Fig. 7 reproduce values obtained from experimental results for glucose efflux from human erythrocytes into an extracellular medium without glucose [13]. Table 1 also shows that $(K_{mapp}/V_m)_{efflux} \approx (K_{mapp}/V_m)_{influx}$ as predicted for facilitated passive diffusion [1].

The results show that different outer and inner apparent affinities (K_{mapp}) might appear even with equal true affinities of the ligand for both transport sites provided that the transconformation equilibrium constants are not equal to one.

3.2 Analyses with Different Dissociation Constants of the Ligand on Both Sides of the Membrane

The previous results, where $K_{De} = K_{Di}$, showed that the increase of initial transport velocities is obtained by increasing the rate constant values and approaching $K_2 = K_4 = 1$. For $K_{De} \neq K_{Di}$, according to (2), if $K_2 = K_4$, they cannot be both equal to 1. Figure 8 shows the initial uptake velocities as a function of K_{De}/K_{Di}. The analyses maintain $K_2 = K_4 \neq 1$.

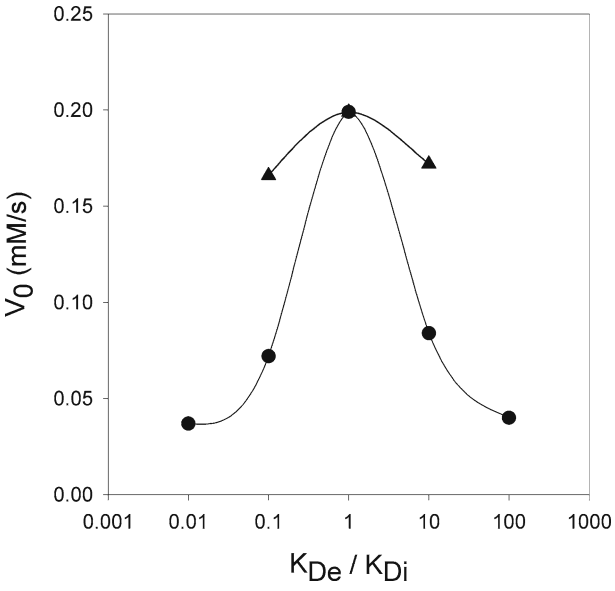

Fig. 8 Initial transport velocities with different affinities of the ligand for the transporter on both sides of the membrane. The initial uptake velocity (V_0) is shown as a function of the K_{De}/K_{Di} relationship. Rate constant values (*filled circles*) are given in Table 2. To avoid the use of some lower rate constant values in analyses with different K_D, compared to that with similar K_D, lower rate constants were replaced by those indicated in parentheses in Table 2 (*filled tringles*)

Table 2 Rate constant values for the analyses shown in Fig. 8

K_{De}/K_{Di}	0.01	0,1	1	10	100
Rate constants					
k_1	1e6	1e6	1e6	1e5(1e6)	1e5
k_{-1}	1e2	1e3	1e3	1e3(1e4)	1e3
k_2	1e3	1e3	1e3	3162	1e4
k_{-2}	1e4	3162	1e3	1e3	1e3
k_3	1e3	1e3(1e4)	1e3	1e3	1e2
k_{-3}	1e5	1e5(1e6)	1e6	1e6	1e6
k_4	1e3	1e3	1e3	3162	1e4
k_{-4}	1e4	3162	1e3	1e3	1e3
Equilibrium constants					
K_1	1e4	1e3	1e3	1e2	1e2
K_2	1e–1	0.3162	1e0	3.162	1e1
K_3	1e–2	1e–2	1e–3	1e–3	1e–4
K_4	1e–1	0.3162	1e0	3.162	1e1

Some results (triangles in Fig. 8) were obtained using the values within brackets. The equilibrium constants are calculated with (1).

The rate constants of the partial reactions are given in Table 2. The figure (circles) shows that maximal initial velocities are obtained when $K_{De} = K_{Di}$.

It could be argued that the decreased initial velocities for K_{De}/K_{Di} equal to 0.1 or 10 are due to the decrease in k_{-3} or k_1, respectively. This is only partially true. The analyses were repeated [Fig. 8 (triangles), Table 2] replacing some rate constants by those shown within brackets. Now, all constants are higher or equal but never lower than those used in the reference condition ($K_{De} = K_{Di}$). Despite the use of some higher rate constant values, initial velocities with different K_D are lower than those obtained with similar K_D.

Taking together the results shown in Figs. 5 and 8, we conclude that for any limited maximal rate constant value, the initial transport velocity is maximal for $K_{De} = K_{Di}$ and $K_2 = K_4 = 1$.

3.3 The *Trans* Effect

Glucose uptake in human erythrocytes, measured with a radioisotopic tracer, is larger in cells containing glucose than in glucose-depleted cells. Also, glucose efflux appears enhanced when the extracellular medium contains glucose. These observations are known as the *trans* effect. The transport of glucose from one side (*cis*) of the membrane is increased by the presence of glucose on the other side (*trans*) [1–3, 7, 13].

3.3.1 Looking for the Trans Effect in an Equilibrated System

To analyze whether the model of alternating conformers can explain the *trans* effect, it is necessary to review the simulation conditions here used. The uptake reaction (Fig. 1) starts by addition of the transported ligand to the system where [Te]/[Ti] = K_4 and [Te] + [Ti] = $[T]_{total}$. Since the model assumes that all rate constants are not modified during transport, the same [Te]/[Ti] relation must be observed at equilibrium, but [Te] + [Ti] decreases because of the appearance of the species Te–Le and Ti–Li and their rise during the transport reaction (Fig. 3b). Therefore, we will always have:

$$[Te]_{equil} < [Te]_0 . \quad (6)$$

To look for the putative *trans* effect, the equilibrium concentrations of the model were calculated. Le was replaced by *Le, a labeled L species at the same concentration. The other non-labeled species were left at their equilibrium concentrations. *Le transport was followed, and a new initial velocity (V_0*) was calculated. This transport has been described as "self-exchange" transport [13]. Here,

$$V_0^* = \left[{}^*\mathrm{Li}\right]_{5\ \mathrm{ms}} - \left[{}^*\mathrm{Li}\right]_{4\ \mathrm{ms}}.$$

Taking into account (6) and the invariance of all k_i values, the transport velocities calculated from the transport of *L in a system containing the unlabelled ligand in equilibrium (V_0*) should be always lower than those calculated from the initial transport of the unlabeled ligand into an initially empty compartment (V_0). This is a consequence of the law of mass action applied to the partial steps participating in the uptake reaction. A similar demonstration applies to efflux analyses. This prediction was tested by numerical simulations using the set of rate constants from Section 3.1.1 (model with maximal initial velocity) and Section 3.1.3.2 (model with influx/efflux asymmetry; data not shown). The results agree with the prediction, indicating that the model of alternating conformers cannot explain the *trans* effect for maximal initial velocities under the simulated conditions.

3.3.2 Simulations of the Trans Effect

In the above section, initial velocities for *Le uptake were calculated starting when *Le replaced equal concentration of Le in an equilibrated system. One might speculate that the eventual appearance of the *trans* effect depends on how the transport velocities are measured.

Figure 9 shows L uptake from a 1 mM L the extracellular compartment into an intracellular compartment with 10 mM L (open circles). The results are compared with

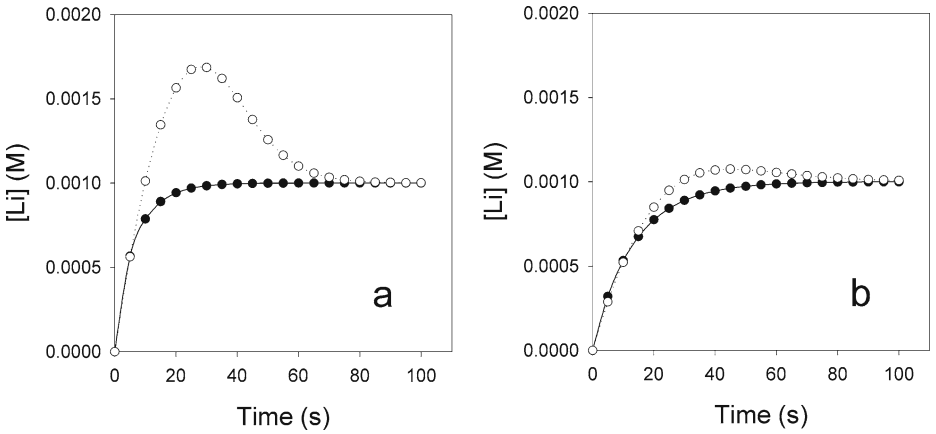

Fig. 9 The demonstration of the *trans* effect depends on how transport velocities are measured. *Open circles*: The system was equilibrated with 10 mM L. Thereafter, 10 mM Le was replaced by 1 mM *Le. The time course of *L uptake is shown. *Filled circles*: Initial conditions: [Le] = 1 mM, [Li] = 0 mM. The time course of [Li] is shown. **a** Rate constants as in Fig. 3. **b** Rate constants as in Fig. 7

L uptake from the same source (1 mM Le) into an empty inner compartment (filled circles). Different rate constant values were used in Fig. 9a, b, as indicated in the legend.

The analysis simulates a system in equilibrium with 10 mM L in both compartments where extracellular Le is suddenly replaced by 1 mM *Le. The figure shows that the initial *Le uptake is favored by the higher internal [Li]. This is explained because upon the change of the extracellular solution, the appearance of the L gradient gives rise to a rapid efflux suddenly increasing Te species through reaction 4, which transiently accelerates reaction 1 and therefore the transport velocity.

The *trans* effect shown in Fig. 9 is a transient phenomenon. Figure 9a shows that at 30 s, the transport is higher when proceeds from a high [L] *trans* compartment. But the figure also shows that differences do not appear at less than 5 s. For these short reaction times, initial velocities are as predicted in Section 3.3.1. For long reaction times, equilibrium is similar for both experimental conditions. Therefore, the *trans* effect might appear in the alternating conformer model of glucose transport depending on how transport velocities are measured.

4 Conclusions

The alternating conformer model of facilitated diffusion explains several properties of glucose transport in erythrocyte membranes. Maximal transport velocities are observed when the dissociation constants of the transported ligand are equal at both sides of the membrane. Equal dissociation constants do not preclude the appearance of the experimentally observed asymmetry between uptake and efflux velocities. The asymmetry is well simulated with different transconformation rate constants, but maximal velocities are obtained with similar equilibrium constants of the transconformation steps and when both approach 1. For initial velocities the model cannot explain the *trans* effect observed in human erythrocyte membranes, but depending on how transport velocities are experimentally measured, the model can explain it.

Appendix 1

Set of differential equations describing the change of the concentrations of the species of the scheme I model. Numerical integration was performed using the program provided in [6].

$$\mathrm{d}[\mathrm{Te}]/dt = k_4 \times [\mathrm{Ti}] + k_{-1} \times [\mathrm{TeLe}] - [\mathrm{Te}] \times (k_1 \times [\mathrm{Le}] + k_{-4})$$

$$d[\mathrm{TeLe}]/dt = \mathrm{k}_1 \times [\mathrm{Te}] \times [\mathrm{Le}] + k_{-2} \times [\mathrm{TiLi}] - [\mathrm{TeLe}] \times (k_{-1} + k_2)$$

$$d[\mathrm{TiLi}]/dt = k_2 \times [\mathrm{TeLe}] + k_{-3} \times [\mathrm{Ti}] \times [\mathrm{Li}] - [\mathrm{TiLi}] \times (k_{-2} + k_3)$$

$$d[\mathrm{Ti}]/dt = k_3 \times [\mathrm{TiLi}] + k_{-4} \times [\mathrm{Te}] - [\mathrm{Ti}] \times (k_{-3} \times [\mathrm{Li}] + k_{-4})$$

$$d[\mathrm{Le}]/dt = k_{-1} \times [\mathrm{TeLe}] - k_1 \times [\mathrm{Te}] \times [\mathrm{Le}]$$

$$d[\mathrm{Li}]/dt = k_3 \times [\mathrm{TiLi}] - k_{-3} \times [\mathrm{Ti}] \times [\mathrm{Li}]$$

References

1. Carruthers, A.: Facilitated diffusion of glucose. Physiol. Rev. **70**, 1135–1176 (1990)
2. Lowe, A.G., Walmsley, A.R.: The kinetics of glucose transport in human red blood cells. Biochim. Biophys. Acta **857**, 146–154 (1986). doi:10.1016/0005-2736(86)90342-1
3. Baker, G.F., Widdas, W.F.: Parameters for 2-O-methyl glucose transport in human erythrocytes and fit of asymmetric carrier kinetics. J. Physiol. **395**, 57–76 (1988)
4. Widdas, W.F.: Inability of diffusion to account for placental glucose transfer in the sheep and consideration of the kinetics of a possible carrier transfer. J. Physiol. **118**, 23–39 (1952)
5. Burrows, R.C., Freeman, S.D., Charlop, A.W., Wiseman, R.W., Adamsen, T.C.H., Krohn, K.A., Spence, A.M.: [^{18}F]-2-fluoro-2-deoxyglucose transport kinetics as a function of extracellular glucose concentration in malignant glioma, fibroblast and macrophage cells in vitro. Nucl. Med. Biol. **31**, 1–9 (2004). doi:10.1016/S0969-8051(02)00449-3
6. Hecht, J.P., Nikonov, J.M., Alonso, G.L.: A BASIC program for the numerical solution of the transient kinetics of complex biochemical models. Comp. Prog. Methods Biomed. **33**, 13–20 (1990). doi:10.1016/0169-2607(90)90018-5
7. Cloherty, E.K., Heard, K.S., Carruthers, A.: Human erythrocyte sugar transport is incompatible with available carrier models. Biochemistry **35**, 10411–10421 (1996). doi:10.1021/bi953077m
8. Challis, J.R.A., Taylor, L.R., Holman, G.D.: Sugar transport asymmetry in human erythrocytes—the effect of bulk haemoglobin removal and the addition of methylxanthines. Biochim. Biophys. Acta **602**, 155–166 (1980). doi:10.1016/0005-2736(80)90298-9
9. Dixon, M., Webb, E.C.: Enzymes, 2nd edn. Longmans, London (1964)
10. Cuppoletti, J.: Transport of ions and nonelectrolytes. In: Sperelakis, N. (ed) Cell physiology—source book, 2nd edn. Academic, San Diego (1995)
11. Nishimura, H., Pallardo, F.V., Seidner, G.A., Vannucci, S., Simpson, I.A., Birnbaum, M.J.: Kinetics of GLUT1 and GLUT4 glucose transporters expressed in Xenopus oocytes. J. Biol. Chem. **268**, 8514–8520 (1993)
12. Baker, G.F., Widdas, R.J.: The asymmetry of the facilitated transfer system for hexose in human red cells and the simple kinetics of a two component model. J. Physiol. **231**, 145–165 (1973)
13. Braham, J.: Kinetics of glucose transport in human erythrocytes. J. Physiol. **339**, 339–354 (1983)